Static and dynamic modeling comparison of an adiabatic compressed air energy storage system

Youssef Mazloum[a], Haytham Sayah[a] and Maroun Nemer[a]

[a]Center for energy efficiency of system (CES), Ecole des Mines de Paris, 5 rue Léon Blum, Palaiseau, France
youssef.mazloum@mines-paristech.fr
haytham.sayah@mines-paristech.fr
maroun.nemer@mines-paristech.fr

Abstract:
Compressed air energy storage plant is a large scale potential energy storage system that provides long-duration energy storage with a small response time. This technology is promising as it creates a balance between production and demand which thereby protects the electric grid. In fact, it makes the electric production of thermal and nuclear power plants more flexible and permits the increase of the contribution of intermittent renewable energies in electricity production.
This paper presents a comparison between the static and dynamic modeling of an adiabatic compressed air energy storage system performed by a computer simulation using "Modelica". The studied storage plant is composed of 3 stages of compression, 3 stages of expansion, an underground cavern for air storage, 6 heat exchangers and a thermal energy storage system.
Unlike the static model, the dynamic model takes into account the mechanical inertia of the turbo-machinery (compressors and turbines), as well as the thermal inertia of the heat exchangers. The developed dynamic model is based on the boundary conditions evolution of the different components of the storage cycle. It allows for examining the global behavior and evolutions of the storage system in time, and thus enables the study of the transient operations including start-up, shut-down, transient evolutions between different states and the continuous working state. Consequently, it enables studying the flexibility of the storage system and its ability to meet the electric grid requirements by evaluating the duration of the transient states. Furthermore, the efficiency losses due to the transient evolutions can be estimated.

Keywords:
Adiabatic compressed air energy storage system (A-CAES), Dynamic modeling, Efficiency, Modelica, Mechanical inertia, Thermal inertia.

1. Introduction:

The balance between supply and demand for electricity in an economic way is the main interest of using electrical energy storage systems. In fact, the electrical production of the thermal and nuclear power plant is not flexible with demand. In addition, for economic and ecological reasons, the contribution of renewable energies in electricity production increases; these energies are intermittent and fluctuate over time depending on meteorological events and thus regardless of power consumption [1, 2]. Furthermore, the peak consumption times impose severe constraints on the electric grid. Therefore, energy storage systems seem interesting to make more flexible the control of the electric production and protect the electric power grid by reducing the frequency variations; they lead also to reduce the electricity cost during the peak consumption [3].

The compressed air energy storage (CAES) system is not a new technology, it is a 40 years old technology. The first utility-scale CAES project [4] was built in 1978 at Huntorf (Germany) with a capacity of 290 MW whereas the second one [5] was built at McIntosh (Alabama, USA) in 1991 with a capacity of 10 MW. Both plants are successfully working for the past nearly 20 years. The largest plant [3] is now under construction in Norton (Ohio) with a power of 2700 MW. The efficiency of the no-adiabatic CAES plants cannot exceed 50% [1, 6]. Hence, research is also in progress to develop an advanced adiabatic compressed air energy storage (A-CAES) system and thus to improve the efficiency of these plants and avoid the use of fossil fuels.

The A-CAES system is a potential and thermal energy storage technology. During off-peak load hours, excess electricity is used to compress air into an underground salt cavern at high pressure (until 200 bars). To increase the efficiency above 50%, heat is recovered from the compressed air and stored under pressure in the form of hot water. During peak load demand hours, compressed air is expanded in the turbines after being heated by the stored hot water to produce electricity [3].

This storage technology has several advantages. First, it allows storing energy on a large scale (several hundreds of MWh) for several hours. Second, it is composed of elements (air, steel and water) with a low environmental impact (recyclable materials) [7]. Third, it does not require the use of fossil fuel. In contrast, it presents some deficiencies since the net efficiency of the A-CAES plants is still low (60% against 80 % for Pumped-storage hydroelectricity) and the storage in an underground cavern depends on geological sites [6].

Many models of the CAES systems have been reported in the literature. Vongmonee and Manyakul [8] have modeled a CAES system to store wind energy in the form of compressed air. Both compression and expansion processes are considered adiabatic since the pressure ratio of these transformations is low (10 bar) [9]. Nielson and Leithner [10] developed an innovative isobaric A-CAES plant with combined cycle. Air is stored in the caverns under fixed pressure by the use of a brine shuttle pond at the surface. Nielson and Leithner [10] studied the dynamic modeling and the calculation results of the simulation of this isobaric system with a detailed dynamic model of the cavern. A novel CAES system for wind turbine has been modeled by Mohsen Saadat and Perry Y. Li [1]. The compression and the expansion are accomplished by an isothermal way and air is stored under high fixed pressure in a dual chamber liquid-compressed air storage vessel. A dynamic model including control laws is developed. Martinez and Mercado [11] studied the modeling and the dynamic performance of a CAES plant that stores the excess energy available in the electric grid. They considered a simple model with isothermal storage tanks. Raju and Khaitan [12] have modeled an air storage-based gas turbine plant by developing Simulink-based models for each component of the storage system. This dynamic model was used to study the case of Huntorf CAES.

The aim of this work is to study the differences between the static and dynamic modeling of an A-CAES plant. The static modeling does not take into account the transient phases of the storage system. On the other hand, the dynamic modeling is developed with sufficient details to take into account the transient phase of each component of the storage plant and hence of the global storage plant. The mechanical inertia of the rotating machines as well as the thermal inertia of the heat exchangers and the hot water tanks are included in the models. The storage system should meet the electric demands as fast as possible to avoid the frequency variations hence the importance of the dynamic modeling, it is relevant to evaluate the time response (duration of the transient state) of the storage system. The dynamic model enables assessing the global behavior and evolution of the storage system in time. Moreover, it permits studying the flexibility of the developed system and evaluating the efficiency losses due to these transient evolutions.

The model is developed using Dymola [13], a software designed to enable a practical modeling of complex systems, such as systems containing mechanical components, hydraulic, thermal...,etc. The simulation language "Modelica" of the Dymola software is an object oriented language. It is a modeling language, rather than a conventional programming language. The associated simulator allows solving the equations system at each time step. This software contains libraries of several fluids, among which was used the air and water libraries [14, 15].

This article is divided into 2 main sections. The first section details the static and dynamic model for each of the individual components (compressors, turbines, cavern, heat exchangers, and hot water tanks) of the A-CAES plant. The second section discusses the global static and dynamic models of the storage system, the simulation results and the efficiency losses due to the transient states.

2. Operation of the A-CAES plant

Fig. 1 depicts the schematic of the A-CAES plant. The developed system mainly includes 3 compressors, 3 coolers, 3 turbines, 3 heaters, an underground cavern and a hot water tank.

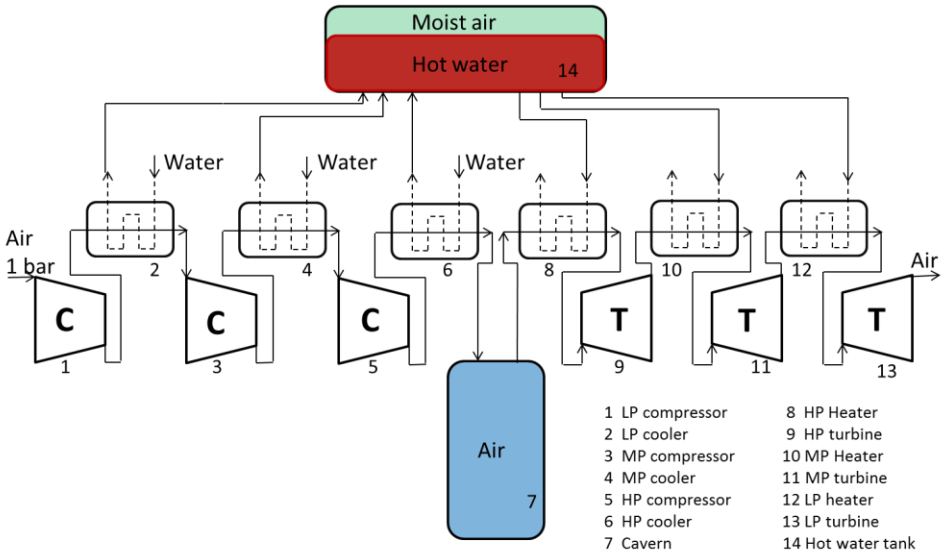

Fig. 1. Schematic of the adiabatic compressed air energy storage plant.

The ambient air is compressed by the compressors using the excesses of electrical energy available on the grid. The air exits the compressors at a high temperature. A heat exchanger is installed at the exit of each compressor to recover the heat of the hot air. This energy is recovered using compressed water. The hot water is then stored in an isolated under pressure tank (around 30 bars). The air leaves the heat exchangers at a low temperature (close to the ambient temperature). Cooling the air increase the compression efficiency due to the high density of the cold air compared to the hot air at the same pressure.

The compressed air is stored in an underground cavern. The pressure inside the cavern increases as the air flows into the last one. The compressors are operated till the cavern pressure reaches the maximum limit.

During the peak demand, the stored air is expanded in the turbines. Air is heated before each of the three turbines through heat exchangers using the stored hot water.

The compression and the expansion processes are divided into three stages to improve the overall efficiency and due to the technological limitations [16].

The next section presents the static modeling of each component of the global A-CAES plant.

3. Static modeling

3.1. Compressor

The compression process is considered polytopic. The model's inputs are the air properties (pressure and enthalpy), the air mass flow rate and the compression ratio where air is assumed to be an ideal gaz. The output enthalpy is evaluated as a function of the isentropic efficiency, as follows:

$$h_{out} = h_{in} + \frac{h_{ise} - h_{in}}{\eta_{ise}} \qquad (1)$$

The compressor electric power is calculated by:

$$P_{elec} = \dot{m} * \frac{h_{out} - h_{in}}{\eta_{elec}} \qquad (2)$$

3.2. Turbine

The expansion process is also considered polytopic. The turbine model is similar to the compressor model. However, the output enthalpy becomes:

$$h_{out} = h_{in} - \eta_{ise}\left(h_{in} - h_{ise}\right) \qquad (3)$$

The turbine electric power produced during the production phase is evaluated as follows:

$$P_{elec} = \dot{m} * \eta_{elec} * \left(h_{in} - h_{out}\right) \qquad (4)$$

3.3. Heat exchanger

Air should be cooled down, in storage mode, in order to protect the compressor from high temperatures and warmed up in discharge mode, in order to protect the turbine from low temperatures. Then, the heat exchangers are necessary for cooling down or heating the air, which improves the overall efficiency. During the air cooling, the water vapor in the air condenses and therefore the air flow leaving the first compressor is dry. The water mass flow rate is calculated by assuming an ideal exchanger:

$$\dot{m}_{water} C_{p\_water} = \dot{m}_{air} C_{p\_air} \qquad (5)$$

The pinch, given as a parameter, allows calculating one of the outlet temperatures. The other outlet temperature is obtained by the energy conservation law using $\dot{m}_{water} * \left|h_{water\_out} - h_{water\_in}\right| = \dot{m}_{air} * \left|h_{air\_out} - h_{air\_in}\right|$ (6):

$$\dot{m}_{water} * \left|h_{water\_out} - h_{water\_in}\right| = \dot{m}_{air} * \left|h_{air\_out} - h_{air\_in}\right| \qquad (6)$$

The pressure loss is considered constant and given as a parameter in the static model.

3.4. Underground cavern

The air is stored under pressure in the underground cavern. The pressure and the temperature in the cavern are determined by the conservation laws of mass and energy. Air is assumed to be an ideal gaz. The mass balance equation can be written as:

$$\frac{d\rho}{dt} = \frac{\dot{m}_{in} - \dot{m}_{out}}{V} \qquad (7)$$

The energy conservation law is written in the following equation [3]:

$$\rho C_p V \frac{dT}{dt} + \dot{m}_{in} C_p \left(T - T_{in}\right) - V \frac{dp}{dt} + h_{cv} S \left(T - T_w\right) = 0 \qquad (8)$$

The term $\rho C_p V \frac{dT}{dt}$ in $\rho C_p V \frac{dT}{dt} + \dot{m}_{in} C_p \left(T - T_{in}\right) - V \frac{dp}{dt} + h_{cv} S \left(T - T_w\right) = 0$ (8)

is the heat accumulation in the stored air, $\dot{m}_{in} C_p \left(T - T_{in}\right)$ is the convective heat flux into the cavern coming from the inlet/outlet air flow, $V \frac{dp}{dt}$ is the compression heat and $h_{cv} S \left(T - T_w\right)$ is the heat transfer with the ambient. The term "$h_{cv}S$" can be approximated experimentally [3].

3.5. Hot water tank

The hot water tank is kept under pressure (≈30 bars) to prevent the evaporation of the hot water. The hot water in the static model is considered as a single volume with one temperature and one pressure.

The inlet enthalpy of the hot water is the average of the inlet enthalpies weighted by the mass flow rate. The inner enthalpy is calculated by $\rho C_p V \frac{dT}{dt} + \dot{m}_{in} C_p \left(T - T_{in}\right) - V \frac{dp}{dt} + h_{cv} S \left(T - T_w\right) = 0$ (8), the terms $V \frac{dp}{dt}$ and $h_{cv} S \left(T - T_w\right)$ are neglected in this case. The static model of the hot water tank takes into account the thermal inertia of the insulated tank. Then, the final enthalpy can be written as follows:

$$M_{water} * \left(h_{in} - h_{final}\right) = M_{steel} * C_{p\_steel} * DT_{cycle} \quad (9)$$

"DT_{cycle}" is the steel's temperature variation between beginning and end of each cycle.

The next section presents the dynamic modeling of each component of the global A-CAES plant.

4. Dynamic modeling

4.1. Compressor

In contrast to the static modeling, the established regime in the dynamic modeling is not instantly established at the machine output, this is because of the mechanical inertia of the impeller and the compressibility of air. These variations of the different physical entities are essential to study an accurate overall behavior of the storage system.

First, the relationship between the angular velocity of the machine's impeller, the motor and the resistant torques is:

$$I \frac{d\omega}{dt} = C_{motor} + C_{resistant} \quad (10)$$

The motor torque is provided by an electric motor and the resistant torque is due to the compressing of the fluid (circuit's load) and the impeller's friction. The electric power consumed by the motor is calculated by:

$$P_{elec} = \frac{C_{motor}\omega}{\eta_{elec}} \quad (11)$$

The impeller resistant torque is evaluated as the friction coefficient by the square of the angular velocity. The motor torque provided allows overcoming the resistant torque of the circuit and the impeller. This resistant torque can be evaluated as follows:

$$P_{resistant} = C_{resistant}\omega = \dot{m}\Delta h + F\omega^2 \quad (12)$$

The enthalpy difference "Δh" is calculated by $h_{out} = h_{in} + \frac{h_{ise} - h_{in}}{\eta_{ise}}$ (**1**).

The flow rate is calculated by an empiric equation provided by the supplier. This characteristic equation is function of the pressure ratio; it takes into account the losses and the flow leakage inside the machine. The characteristic equation changes with the angular velocity of the machine, it is evaluated by the similarity laws. For a compressor, this equation has an exponential form [17] as shown below:

$$R = (1 - R_i)(1 - \exp(k\dot{m}_i))^{-1}(1 - \exp(k\dot{m})) + R_i \quad (13)$$

The intermediate compression ratio "Ri" is calculated by a third order polynomial equation having the square of the angular velocity as a variable and the intermediate mass flow rate "$\dot{m}_i$" is calculated by the similarity laws [20].

4.2. Turbines

The turbine response to the power demand is not instant due to the mechanical inertia of the turbine and the properties of the fluid. Therefore, it is essential to develop a dynamic model of the turbine which allows, according to the boundary conditions of the turbine, calculating the produced electrical power. This study is very important to determine the response time of the storage system for a power demand and its ability to stabilize the grid power. The functioning of the turbine depends on the angular velocity of the shaft, the flow rate and the fluid characteristics (the enthalpy and the pressure).

The enthalpy variation is calculated by $h_{out} = h_{in} - \eta_{ise}\left(h_{in} - h_{ise}\right)$ (**3**) and the angular velocity is evaluated by (10). The motor torque is produced in this case by the flow crossing the turbine; this torque is calculated based on equation $P_{motor} = \dot{m}\Delta h = C_{motor}\omega$ (14). The electric power is calculated from the motor power using the mechanical and the electrical efficiencies. The resistant torque is evaluated by $P_{elec} = C_{resistant}\omega$ (15).

$$P_{motor} = \dot{m}\Delta h = C_{motor}\omega \qquad (14)$$

$$P_{elec} = C_{resistant}\omega \qquad (15)$$

The dynamic model of the turbine includes a control system which adjusts the flow rate by using a control valve. First, the control system regulates the flow rate to reach the operating speed. This speed depends on the electric generator properties and the grid frequency. After reaching the operation speed, the control system regulates the flow rate to touch the desired power imposed by the electric grid.

4.3. Exchangers

The thermal inertia of the heat exchangers increases the heat losses especially during the cold start. The homogenization of the temperature during standby mode is important yet. The temperature difference between the inlet and the outlet of the heat exchanger (≈150°C) creates a thermal flux trying to homogenize the heat exchanger. This phenomenon reduces the air temperature at the exit of the heater heat exchanger, the water temperature at the exit of the cooler heat exchanger and therefore reduces the efficiency of the system during the transient state. The dynamic modeling of the heat exchanger is essential to take into account these losses. The heat exchanger model consists of modeling the heat transfer between two fluids through a tube in tube heat exchanger. This model takes into account the thermal inertia of the heat exchanger and all heat losses, whether to the surrounding or by homogenization of the temperature. The exchanger is assumed to be Two-dimensional.

The heat exchanger is meshed, the temperature of each cell is evaluated by the conservation energy law detailed as follows:

$$\sum q_i + \dot{m}\Delta h + MC_p\frac{dT}{dx} = 0 \qquad (16)$$

Where "$\sum q_i$" is the sum of the heat quantities exchanged with the mesh.

The convective heat transfer coefficient between the fluid (air or water) and the pipe is evaluated by correlations [19] which are function of the numbers of Reynolds, Prandtl and Nusselt.

The pressure drop is evaluated by [20]:

$$\Delta p = f\frac{L}{D_h}\frac{\rho v|v|}{2} \qquad (17)$$

4.4. Hot water tank

The energy required to heat the water tank, the homogenization of the water temperature and the waste heat are essential to quantify. The dynamic modeling of the hot water tanks takes in accounts all these heat losses. The inside pressure of the water tank is a result of saturation between the water and the moist air. The model is similar to the heat exchanger model. However, the conservation energy low is defined as follows:

$$\sum q_i + \dot{m}\Delta h + MC_p \frac{dT}{dx} + V\frac{dp}{dt} = 0 \qquad (18)$$

The humidity ratio of the moist air is calculated as follows [21]:

$$W = 0.6431\frac{p_{sat}}{p - p_{sat}} \qquad (19)$$

The mass balance equation of water is calculated by $\frac{d\rho}{dt} = \frac{\dot{m}_{in} - \dot{m}_{out}}{V}$ (7). In storage phase, the steam condenses as the hot water filling and the pressure increases slowly. By against in production phase, water evaporates as the hot water emptying and the pressure decreases. The result pressure is near to the saturation pressure.

4.5. Air tank

The dynamic model of the underground cavern is similar to the static model.

5. Static and dynamic simulations

5.1. Simulation results

The global compressed air energy storage model is simulated for several storage and production cycles. The whole cavern is dimensioned as Huntorf Cavern [3, 22]. The cavern wall temperature and the initial air temperature are assumed to be equal to 25°C.

The key data of the Huntorf plant is shown in Table 1. This data is used for the simulation of the static and dynamic model of the adiabatic storage system.

Table 1. Key data of the Huntorf plant

Parameters	Values
Cavern volume	300 000 m^3
Compressor mass flow rate	≈ 108 Kg/s
Turbine mas flow rate	≈ 400 Kg/s
Initial pressure	46 bar
Final pressure	≈ 66 bar
Maximum pressure reduction rate	10 bar/h
Storage time	12 hours
Production time	3 hours

Fig. 2 depicts the variation of both the static and dynamic internal cavern pressures, this figure shows the progress of the static pressure on the dynamic due to the neglect transient state. The dynamic compressor needs about 40 seconds before delivering air in the cavern. This results in a greater static pressure in the static model than the dynamic model (the difference is about 0.77 %). The dynamic turbine requires also about 5 minutes before it gets to its full power capacity. At first, the pressure decreases more in the static model than the dynamic model and becomes later approximately equal in both models. The transient phases of the turbo machines are not negligible, the system could not neither consume nor produce instantly the desired grid power.

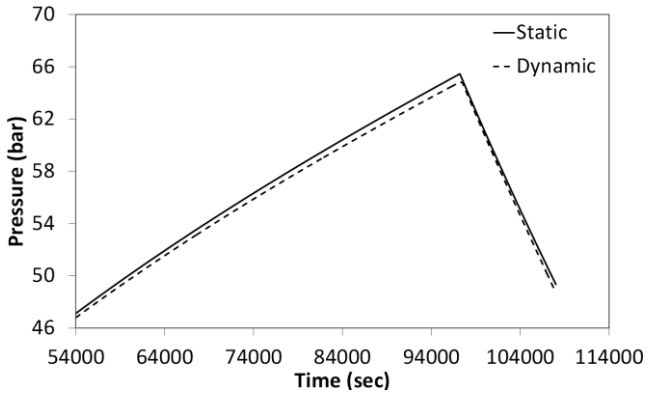

Fig. 2. Static and dynamic internal pressures of the cavern.

The polytropic efficiency (Fig. 3Fig. 4) is function of the mass flow rate and the angular velocity. The optimum polytropic efficiency of the all compressors and turbine stages used is equal to 87%. The electric efficiencies are assumed to be 96% for the compressor and the turbine. The limitation of cycling between 46 and 66 bar aims to work in the optimal performance area of turbines and compressors.

Fig. 5 shows the compressor mass flow rates of the static and dynamic simulations. The static flow rate reaches the steady state instantly. By contrast, the transient state neglected in the static modeling is taken into account in the dynamic modeling. So the dynamic flow rate remains zero until the compressor outlet pressure becomes greater than the cavern's pressure (about 38 seconds), and then the curve rises to reach the static flow rate in about 104 seconds. As shown in **Erreur ! Source du renvoi introuvable.**, the dynamic power increases at first rapidly to overcome the compressor inertia. Then the velocity increases, the inertia effect goes down and the consumed power decreases. Once the valve is opened, the consumed power increases again to touch the static value in about 142 seconds. Therefore, the compressors take more than 2 minutes to be able to consume all the excess energy on the electric grid.

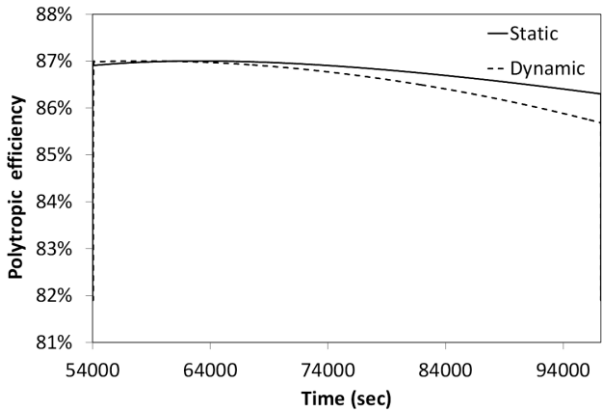

Fig. 3. Static and dynamic polytropic efficiencies of the compressor low pressure stage.

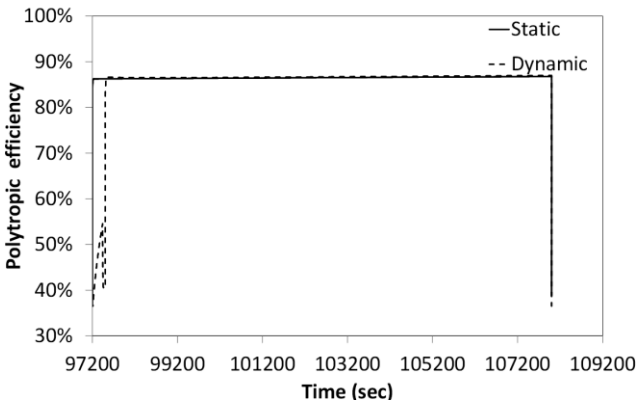

Fig. 4. Static and dynamic polytropic efficiencies of the turbine high pressure stage.

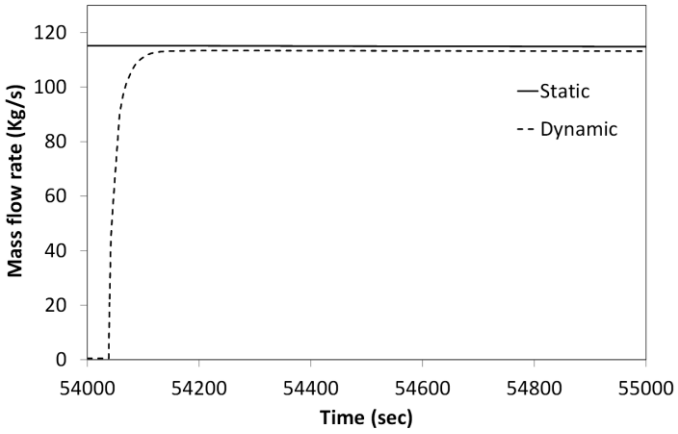

Fig. 5. Static and dynamic compressor mass flow rates.

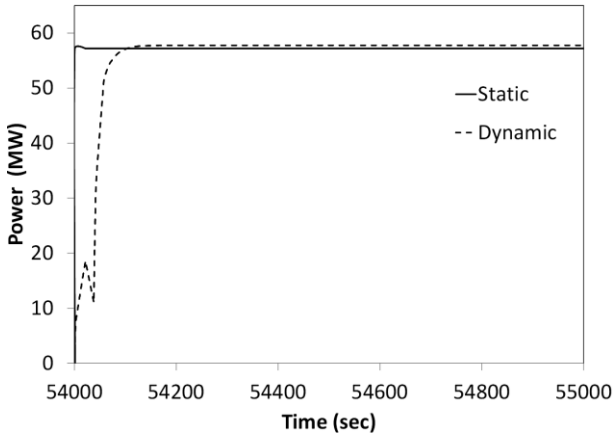

Fig. 6. Static and dynamic compressor powers.

The turbine transient state is formed of 2 parts. As shown in Fig. 7, the dynamic mass flow rate increases first to overcome the turbine inertia and the friction torques in order to reach the set point velocity. Once the set point velocity is attained, the inertia effect is reduced, as a result the mass flow rate decreases and a minimum value of about 15.7 Kg/s still needed to overcome the friction torques. When the turbine is coupled to the electric grid, the flow rate raises rapidly to retouch the set point speed and produce the imposed power. **Erreur ! Source du renvoi introuvable.** shows the static and dynamic turbine powers, the dynamic power increases rapidly after 5 minutes of the production phase beginning. Then, it decreases with the reduction of the velocity before reaching of the static power again. The turbine transient state takes approximately 5 minutes to attain the angular velocity set point and be able to be synchronized with the electric grid. For that reason, the storage system isn't able to meet the electric demands instantaneously.

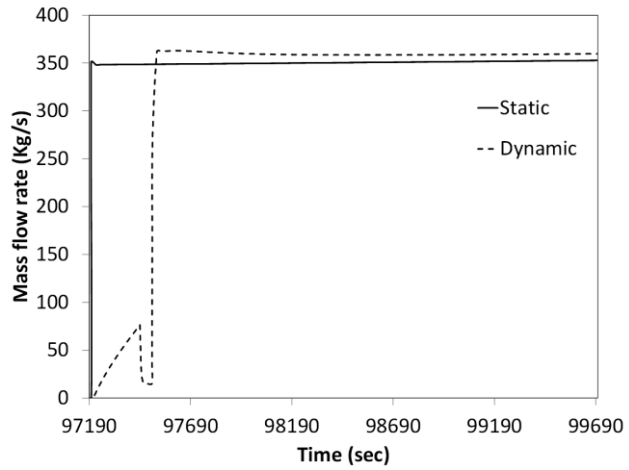

Fig. 7. Static and dynamic turbine mass flow rates.

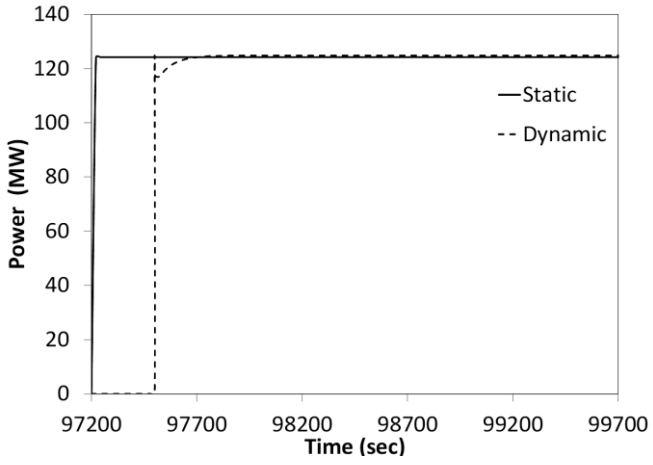

Fig. 8. Static and dynamic turbine powers.

As shown in Fig. 9, the water output temperatures of the dynamic coolers heat exchangers increase initially from the initial to the static temperature. The transient state duration depends on the exchanger inertia (steel mass), it is about 30 minutes in this case. During standby mode (production mode), the temperature homogenization and the waste heat cause the drop of the output water temperature about 10°C. At the beginning of the second period simulation, the temperature decreases firstly (unlike the static state) according to the air input temperature. The coolers inertia facilitates the air cooling at the beginning, then they don't affect the response time of the storage system. However, they increase the efficiency loss by storing cold water in the hot water tanks at the beginning.

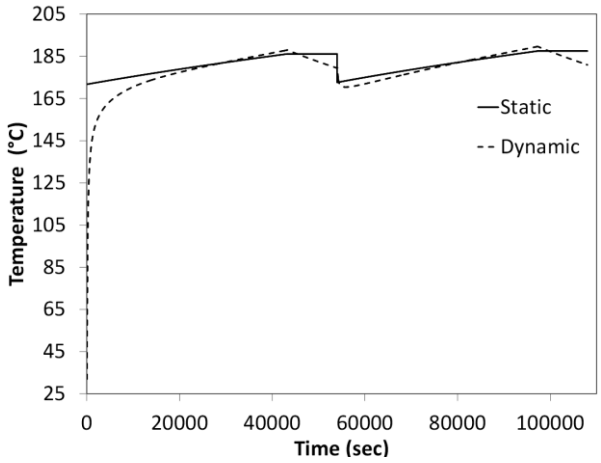

Fig. 9. Static and dynamic water output temperatures of the low pressure cooler.

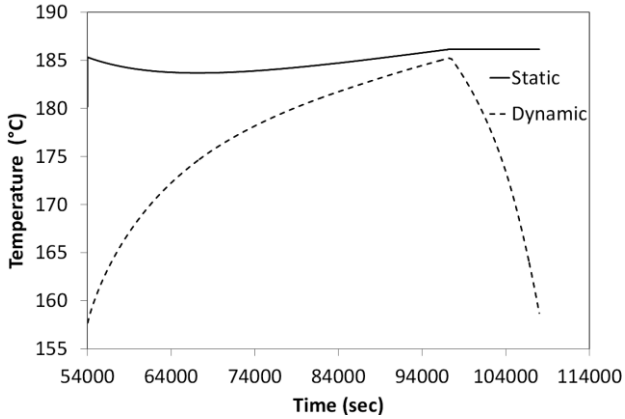

Fig. 10. Static and dynamic temperatures of the hot water tank.

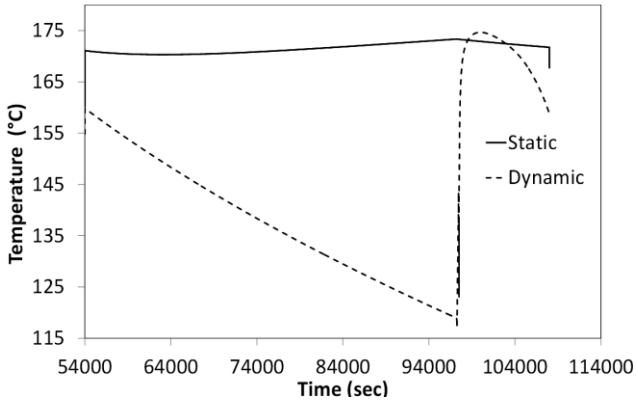

Fig. 11. Static and dynamic air output temperatures of the high pressure heater.

Fig. 10 shows the water inlet/outlet temperatures in the hot water tank during the second period of simulation. During storage phase, water temperature increases slowly to overcome the thermal inertial and reheat the cold water before touching the static temperature. During production phase, the water evaporation as the pressure decreases and the waste heat provoke the temperature drop. The static temperature is approximately constant in this mode.

The waste heat and the temperature homogenization provoke the air outlet temperature drop of the heaters (**Erreur ! Source du renvoi introuvable.**) during storage mode (about 40°C). It varies during production mode depending on the air mass flow rate. The transient state duration is about 15 minutes. During start-up of the turbines, hot air is needed to prevent a low air temperature at the output hence the importance of keeping warm exchangers.

5.2. Efficiency comparison

The net efficiency of the developed system is calculated by (18):

$$\eta_{net} = \frac{E_{Turbines}}{E_{Compressors}} \qquad (20)$$

The static and dynamic net efficiencies of the storage system are presented in Table 2.

Table 2. Net efficiencies of the adiabatic storage system

Static efficiency	66 %
Dynamic efficiency of the first cycle	63.9 %
Dynamic efficiency of the second cycle	64.7%.

The start-up of the storage system with cold exchangers and hot water tanks is the origin of the difference efficiencies between the first and the second period of simulation (0.8 %).

The difference between the static and dynamic efficiencies is the dynamic losses (1.3 %). The mechanical inertia of the turbo machines causes a loss of about 0.2 %. The energy consumed to start-up the compressors and the waste mass flow rate expanded during the transient phase of the turbines are the origin of these losses. The thermal inertia of the heat exchangers costs 0.4 % of the net efficiency, it is the lost energy used to warm up the heat exchangers during the transient states and the losses by temperature homogenization during the standby mode. The thermal inertia of the hot water tanks, the water evaporation losses and the waste heat are the origin of the 0.7 % losses which remains.

6. Conclusion

We presented in this paper a detailed study about both the static and dynamic modeling of an adiabatic compressed air energy storage system. The static modeling describes the global behavior of the system by neglecting its inertia whereas a dynamic model, taking into account the inertia of the system, is essential to study the behavior of the system at the start up, shut down and in several operations. The latter allows simulating the dynamic operations and identifying the ability of the storage system to meet the electric requirements as a function of its inertia. The simulations are realized using Huntorf caverns as a case study.

In storage mode, the compressors need approximately 140 seconds to get to the steady state and pump the optimal flow in the caverns. Consequently, the storage system is not able to consume instantly all the excess energy from the electric grid.

In production mode, the turbines require 5 minutes to be able to synchronize with the electric grid and produce the desired electric power. Furthermore, the heaters necessitate also 15 minutes to exceed the transient state. By consequently, the system cannot meet the electric requirements immediately; the minimum 5 minutes needed may negatively influence the grid frequency during the peak demand.

The inertias of the system cause a loss of about 1.3% distributed between the mechanical inertia of the turbo machines, the thermal inertia and the waste heat of the exchangers and the hot water tanks.

Nomenclature

A-CAES	adiabatic compressed air energy storage
CAES	compressed air energy storage
C	torque
C_p	specific heat capacity, (J/kg.K)
D_h	hydraulic diameter, (m)
E	energy, (J)
F	Impeller friction coefficient
f	linear pressure loss coefficient
h	mass enthalpy, (kJ/kg)
h_{cv}	heat convection coefficient, ($W/m^2.K$)
I	Moment of inertia, ($Kg.m^2$)
k	constant
L	length, (m)
m	mass flow rate, (kg/s)
M	mass, (Kg)
P	power, (W)
p	pressure, (Pa)
p_{sat}	saturation pressure, (Pa)
q	quantity of heat, (W)
R	compression ratio
S	cross sectional area, (m^2)
t	time, (sec)
T	temperature, °C
V	Volume, (m^3)
v	velocity, (m/s)
w	humidity ratio, (kg/kg)
x	abscissa, (m)

Greek symbols

η	efficiency, %
ρ	density, (Kg/m^3)
ω	angular velocity, (rad/s)
Δ	difference

Subscripts

elec	electric
i	intermediate

in	input	out	output
ise	isentropic	w	water

References

[1] Saadat M. and Y.Li P., Modeling and Control of a Novel Compressed Air Energy Storage System for Offshore Wind Turbine. 2012 American Control Conference Fairmont Queen Elizabeth, Montréal, Canada June 27-June 29, 2012.

[2] Chedid R, Salameh S, Karaki S, Yehia M, Al-Ali R. Optimization of Electrical Distribution Networks Fed by Conventional and Renewable Energy Sources. International Journal of Energy Research 1999; 23(9):751-763.

[3] Khaitan S.K. and Raju M., Dynamic Simulation of Air Storage–Based Gas Turbine Plants. International Journal of Energy Research 2013; 37:558-569.

[4] Hoffeins H. Huntorf air storage gas turbine power plant, In Energy Supply, Brown Boveri Publication DGK 90 202 E, 1994 http://www.kraftwerkwilhelmshaven.com/pages/ekw_de/Kraftwerk_Wilhelmshaven/Mediencenter/_documents/BBC_Huntorf_engl.pdf

[5] Hounslow DR, Grindley W, Louglin RM, Daly J, The development of a combustion system for a 110 MW CAES plant. Journal of Engineering for Gas Turbines and Power 1998; 120:875-883.

[6] ENEA CONSULTING, " Enjeux, solutions techniques et opportunités de valorisation". Le stockage d'énergie, 18 (Mars 2012).

[7] Lemofouet S. and Rufer A., Hybrid energy storage systems based on compressed air and supercapacitors with maximum efficiency point tracking. 2005 IEEE European Conference on Power Electronics and Applications; 53:1105-1115.

[8] Vongmanee V, Monyakul V., A Modeling of Small-Compressed Air Energy Storage System (Small-CAES) for Wind Energy Applications. GMSARN International Conference on Sustainable Development: Issues and Prospects for the GMS. 12–14 Nov. 2008.

[9] Vongmanee V., Monyakul V., A new concept of small-compressed air energy storage system integrated with induction generator. Sustainable Energy Technologies, 2008. IEEE International Conference ; 866-871.

[10] Nielsen L, Leithner R. Dynamic Simulation of an Innovative Compressed Air Energy Storage Plant— Detailed Modeling of the Storage Cavern. WSEAS TRANSACTIONS on POWER SYSTEMS 2009; 4(8):253–263.

[11] Martinez M, Mercado PE, Dynamic Performance of Compressed Air Energy Storage (CAES) Plant for Applications in Power Systems. Latin America: IEEE/PES Transmission and Distribution Conference and Exposition, 2010.

[12] Raju M, Khaitan S. Modeling and simulation of compressed air storage in caverns: a case study of Huntorf CAES plant. Applied Energy 2012; 89(1):474–481.

[13] Dassault systemes, the official web site of Dymola, http://www.3ds.com/products-services/catia/capabilities/modelica-systems-simulation-info/dymola

[14] Cooper J. R., Dooley R. B., The International Association for the Properties of Water and Steam, Lucerne, Switzerland, August 2007.

[15] McBride B.J., Zehe M.J., and Gordon S. (2002): NASA Glenn Coefficients for Calculating Thermodynamic Properties of Individual Species. NASA report TP-2002-211556

[16] Lemofouet-Gatsi S., investigation and optimisation of hybrid electricity storage systems based on compressed air and supercapacitors. Institut des sciences de l'énergie, octobre 2006.

[17] Schalbart P., "Modélisation du fonctionnement en régime dynamique d'une machine frigorifique bi-étagée à turbo-compresseurs-Application à sa régulation", Institut national des sciences appliquées de Lyon, December 2006, 195 (61-73).

[18] Balje, O.E., Turbomachines, Wiley, 1981, New York, NY.

[19] F. Incropera, D. Dewitt, Fundamentals of Heat and Mass Transfer. School of mechanical engineering, Perdue University, 1996,886 (420-515).

[20] I.E. Idelchik, "Handbook of Hydraulic Resistance", 3rd Edition, 1993, 788 (75-87).

[21] Chaddock, J.B. 1965. Moist air properties from tabulated virial coefficients. *Humidity and moisture measurement and control in science and industry* 3:273. A. Wexler and W.A. Wildhack, eds. Reinhold Publishing, New York.
[22] Crotogino F., Mohmeyer K. and Scharf R., Huntorf CAES: More than 20 Years of Successful Operation. Spring 2001 meeting Orlando, Florida, USA, 15-18 April 2001.